

Contents lists available at ScienceDirect

Theoretical Computer Science

www.elsevier.com/locate/tcs



Probabilistic reachability for multi-parameter bifurcation analysis of cardiac alternans



Md. Ariful Islam^{a,*}, Rance Cleaveland^b, Flavio H. Fenton^c, Radu Grosu^d, Paul L. Jones^e, Scott A. Smolka^f

- ^a Carnegie Mellon University, Pittsburgh, PA, USA
- ^b University of Maryland, College Park, MD, USA
- ^c Georgia University of Technology, Atlanta, GA, USA
- ^d Vienna University of Technology, Vienna, Austria
- ^e U.S. Food and Drug Administration, Silver Spring, MD, USA
- f Stony Brook University, Stony Brook, NY, USA

ARTICLE INFO

Article history: Received 13 April 2017 Received in revised form 10 January 2018 Accepted 3 February 2018 Available online 12 February 2018

Keywords:
Probabilistic reachability
Cardiac modeling
Cardiac alternans
Bifurcation analysis
Formal methods
Hybrid systems

ABSTRACT

Using a probabilistic reachability-based approach, we present a multi-parameter bifurcation analysis of electrical alternans in the two-current Mitchell–Schaeffer (MS) cardiac-cell model. Electrical alternans is a phenomenon characterized by a variation in successive Action Potential Durations generated by a cardiac cell or tissue. Alternans are known to initiate re-entrant waves and are an important physiological indicator of an impending life-threatening arrhythmia such as ventricular fibrillation. The multi-parameter bifurcation analysis we perform identifies a bifurcation hypersurface in the MS model parameter space, such that a small perturbation to this region results in a transition from highly likely alternans to highly likely non-alternans behavior.

Our approach to this problem rests on encoding alternans-like behavior in the MS model as a five-mode, multinomial hybrid automaton. To perform multi-parameter bifurcation analysis of cardiac alternans, we first treat the parameters in question as bounded random variables. We then apply a sophisticated guided-search-based probabilistic reachability analysis to compute a bounded bifurcation region (possibly very tight) that contains the bifurcation hypersurface (BH). Our probabilistic reachability analysis uses a technique that combines a δ -decision procedure with statistical tests. In the process of computing the bifurcation region, we further partition the parameter space into two more regions such that any valuation chosen from one of the regions will either produce alternans or non-alternans behavior with a probability greater than a user-defined threshold.

© 2018 Elsevier B.V. All rights reserved.

1. Introduction

Cardiac arrhythmia, associated with abnormal electrical activities in the cardiac tissue, remains one of the leading causes of death in industrially developed countries. In the US alone, 300,000 to 500,000 deaths per year can be attributed to cardiac arrhythmias [8]. A number of studies have shown that *alternans*, a phenomenon characterized by a period-doubling

E-mail address: mdarifui@cs.cmu.edu (Md.A. Islam).

st Corresponding author.

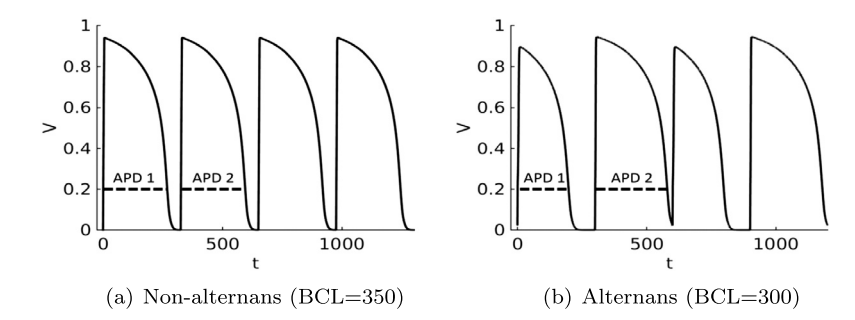


Fig. 1. Voltage time series for Mitchell–Schaeffer model using parameter values $[\tau_{in}, \tau_{out}, \tau_{open}, \tau_{close}, V_g] = [0.3, 6, 20, 150, 0.1]$. Threshold value used to compute the APD is $V_T = 0.2$. (a) Time series does not meet definition of alternans since APD1 = APD2. (b) Time series meets definition of alternans since APDs alternate in length (short, long, short, long).

bifurcation where, while cells are paced at a constant period, their response has different dynamics between even and odd beats, with one long action potential following a short one [36] (see Fig. 1), represent an important physiological indicator of cardiac arrhythmias such as ventricular fibrillation (VF) and ventricular tachycardia (VT) [11,30,43–45,48]. Alternans are also known to destabilize or initiate reentrant waves [22].

The cardiac device known as *implantable cardioverter defibrillator (ICD)* helps to prevent sudden cardiac death (SCD) [13, 33,37,40]. The patients who are at high risk of developing life-threatening VT and VF are only chosen to be implanted with ICDs, as unnecessary implants can induce some unwanted side-effects [38]. According to the guidelines provided by the American Heart Association (AHA) and European Society of Cardiology (ESC), cardiac alternans, in particular T-Wave alternans (TWA), plays an important role to select such critical patients [25]. Though, in this paper, we analyze cellular alternans, Chen et al., via numerical and experimental studies, show that cellular alternans are linked with TWA [12]. Thus understanding the mechanism of cellular alternans may lead to a better understanding of TWA, which, in turn, will help improved patient selection for ICD implants.

An important component of cardiac electrodynamic modeling is the ability to understand and predict qualitative changes that take place in the dynamics as model parameters are varied [1,15,47]. One well-known change involves a transition to alternans from the normal (non-alternans) 1:1 response.

About 100 mathematical models [16] have been developed to recreate and study, to varying degrees of complexity, the electrical dynamics of a cardiac cell (i.e., cardiomyocyte). An appealing one in terms of its mathematical tractability is the Mitchell Schaeffer (MS) model [39], which represents the cellular electrodynamics using only two state variables: a voltage variable ν representing the trans-membrane potential, and a gating variable h capturing the internal ionic state of the cell.

It is well known that the region of the restitution curve (RC), a nonlinear mapping between the *action potential dura*tion (APD) and the preceding *diastolic interval* (DI), having a slope greater than 1 can produce oscillation in APD via Hopf bifurcation [29]. Such theoretical bifurcation analysis, however, is generally not possible, as the analytical form of the RC is typically unknown. Even though through various pacing protocols it is possible to compute an approximation of the RC, it could differ from protocol to protocol [14]. Therefore, depending on the pacing protocol used to approximate the RC, the RC-based bifurcation analysis could vary significantly.

Rather than relying on the RC, we presented a single-parameter bifurcation analysis of cardiac alternans in the MS model based solely on the model dynamics. The bifurcation analysis we performed determined, for each parameter τ of the MS model, a tightly bounded region that contains the bifurcation point (BP)¹ in the range of τ such that a small perturbation to this region results in a transition from alternans to non-alternans behavior. Our approach to this problem relied on encoding the alternans-like behavior in the MS model as an 11-mode hybrid automaton and then performing a guided-search-based reachability analysis on this HA using the dReach tool [32], which uses the dReal SMT solver [20].

The algorithm of [26] determines the bifurcation region by partitioning the parameter space recursively in a binary-search-like manner until it bounds the BP in a small region. In each step of the recursive search, the algorithm divides the current partition if it is bigger than a prescribed size or the algorithm, with a *certainty*, cannot rule out the possibility that the partition may contain a BP. Thus, the recursive search may take a considerable amount of time. Moreover, the number of partitions in the recursive search could grow *exponentially* with the number of the parameters. Thus, the dReach-based bifurcation analysis may not scale well in a multi-parameter setting.

Main contributions. In this paper, we propose a new technique for bifurcation analysis by reducing this problem into a *probabilistic reachability* problem. The computational effort required to perform bifurcation analysis is prohibitively expensive. Only some preliminary work in that direction being reported so far [23]. Instead of performing multi-parameter analysis, the standard procedure first computes a bifurcation diagram, i.e., curves of equilibrium solutions, by varying one parameter while keeping all the other parameters constant. By repeating this, a series of bifurcation diagrams can be obtained. In con-

¹ For a single-parameter analysis, the bifurcation hypersurface is a point.

trast, we propose a novel method for computing the bifurcation surface without the need of computing multiple bifurcation diagrams. Though, instead of certainty, our approach provides a probabilistic guarantee whether a parameter valuation will produce alternans or non-alternans, it is highly scalable for multi-parameter bifurcation analysis of nonlinear dynamical systems. Moreover, the probability at which it may provide the guarantee can be controlled by user-defined thresholds as well as by changing the parameters of the statistical tests at the expense of increasing the model-exploration time.

Similar to [26], we first encode alternans behavior as an HA. We, however, construct a smaller-sized HA by reducing the number of modes from 11 to 5. We then treat all the parameters in question as bounded random variables in the HA. Finally, we apply a sophisticated recursive guided-search-based probabilistic reachability analysis in the HA using the sReach tool [49], which combines the dReach and statistical tests.

We start by considering the entire parameter space as a single partition. In each step of the recursive search, we first estimate the probability of producing alternans by the current partition. We further divide the partition, if the estimated probability is within the user-defined range $[P_l, P_h]$ (e.g., [0.1, 0.9]) or it is bigger than a prescribed size. Applying this strategy, our method is able to bound the BH in a tight bounded region as well as two more regions: 1) alternans region that produces alternans behavior with probability greater than $(1 - P_l)$.

Paper organization. This paper is organized as follows. Section 2 presents the MS model and a brief overview of the dReach and sReach tools that we use to perform reachability analysis. Section 3 represents the MS model as an HA and then extends the MS HA to encode alternans behavior. Section 4 formally defines multi-parameter bifurcation analysis of alternans, and describes our approach to this problem, which is based on reducing it to a probabilistic reachability problem for the HA that encodes alternans. Section 5 presents our results for the bifurcation analysis of various combinations of 2 and 3 parameters of the MS model. Section 6 considers related work. Section 7 offers our concluding remarks and directions for future work.

2. Background

2.1. The Mitchell-Schaeffer model

The Mitchell-Schaeffer model is an activator-inhibitor system that describes the electrical dynamics of a ventricular myocyte. The model involves two coupled, nonlinear ordinary differential equations of the form:

$$\dot{v} = I_{in}(v, h) + I_{out}(v) + I_{s}(t)$$

$$\dot{h} = \begin{cases}
\frac{1-h}{\tau_{open}} & v < V_g \\
\frac{-h}{\tau_{ther}} & v \ge V_g
\end{cases}$$
(1)

where v(t) is the transmembrane voltage and h(t) is a gating variable (as in a voltage-gated ion channel [16]). The voltage ranges from -85 to 20 mV in a real cardiac cell, but has been scaled to the range [0, 1] in the MS model, and is expressed as the sum of three currents: an inward current, outward current and stimulation current. The inward current $I_{in}(v,h) = hv^2(1-v)/\tau_{in}$ is designed to replicate the behavior of fast-acting gates found in more complex models. The outward current $I_{out}(v) = -v/\tau_{out}$ is ungated and represents the currents that act to decrease the membrane voltage. The strength of each respective current is controlled by the timing parameters τ_{in} and τ_{out} .

The stimulus current I_s is an externally applied current which is used to periodically excite an action potential (AP) in the cell. It is applied every BCL (Basic Cycle Length) milliseconds for a duration of τ_s milliseconds.

The gating variable h(t) is dimensionless and scaled between 0 and 1. Parameters τ_{close} and τ_{open} are time constants that control the opening and closing of the h-gate, and V_g is the "critical" gating voltage; i.e., the voltage required to generate an action potential. The four time constants in the model are used to control the four phases of the cardiac action potential.

For certain parameter values, the Mitchell–Schaeffer model can exhibit alternans, a state which successively exhibits alternating short–long values of the APD. An example of alternans and non-alternans behavior in the voltage time series is shown in Fig. 1.

2.2. The dReach tool

dReach [32] is a bounded-time reachability analysis tool for nonlinear hybrid systems. It takes a *hybrid automaton* (HA) \mathcal{H} , reachability properties \mathcal{P} , a numerical error bound $\delta \in \mathbb{Q}^+$, and an unrolling depth $k \in \mathbb{N}$ as inputs. It then encodes a bounded-reachability problem for a hybrid automaton as a first-order formula over the reals and solves the formula using the delta-decision SMT solver dReal [21]. There are two possible outputs from the dReach tool:

- unreachable: dReach confirms that there is no trace satisfying the reachability properties up to k discrete jumps.
- δ -reachable: dReach shows that there exists a trace ξ satisfying the reachability properties if we consider a user-specified numerical perturbation $\delta \in \mathbb{Q}^+$ in \mathcal{H} . The tool also provides a feature to visualize this trace.

We note that the bounded-time reachability problem for nonlinear hybrid automata is undecidable [4]. The tool is implemented in the framework of delta-complete analysis for bounded reachability of hybrid systems [19], which provides an algorithm for the originally undecidable problem by using approximation (the use of δ in the analysis).

2.3. Probabilistic reachability analysis using SReach

SReach [49] is a probabilistic bounded-time reachability analyzer for two classes of models of stochastic hybrid systems: (nonlinear) hybrid automata with parametric uncertainty, and probabilistic hybrid automata with additional randomness. It takes a stochastic hybrid automaton \mathcal{H}_s , reachability properties \mathcal{P} , a numerical error bound $\delta \in \mathbb{Q}^+$, an unrolling depth $k \in \mathbb{N}$, and a chosen statistical testing method as inputs. It then encodes uncertainties in the given stochastic hybrid automaton \mathcal{H}_s using random variables, and samples them according to the given distributions. For each sample, a corresponding intermediate HA is generated by replacing random variables with their assigned values. Then, the δ -complete analyzer dReach [18] is utilized to analyze each intermediate HA M_i , together with the desired precision δ and unfolding depth k. The analyzer returns either unsat or δ -sat for M_i . This information is then used by a chosen statistical testing procedure to decide whether to stop or to repeat the procedure, and to return the estimated probability.

SReach supports a number of hypothesis testing and statistical estimation techniques (see [49] for details). All methods produce answers that are correct up to a precision that can be set arbitrarily by the user. SReach can answer two types of questions:

- With hypothesis testing methods, SReach can answer qualitative questions, such as "Does the model satisfy a given reachability property in *k* steps with probability greater than a certain threshold?"
- With statistical estimation techniques, SReach can offer answers to quantitative problems. For instance, "What is the probability that the model satisfies a given reachability property in *k* steps?"

SReach can also handle additional types of interesting problems, including the *model validation/falsification* problem with prior knowledge, the *parameter synthesis* problem, and the *sensitivity analysis*, by encoding them as bounded reachability problems.

3. Hybrid automata for the MS model and alternans

In this section, we represent the MS model as a hybrid automaton (HA) and extend this automaton to encode alternans.

3.1. Hybrid automaton (\mathcal{H}_{M}) for the MS model

The stimulus current $I_s(t)$ in Eq. (1) is a periodic square-wave signal defined in each AP cycle as:

$$I_{s}(t) = \begin{cases} I_{stim} & \text{if } t \leq \tau_{s} \\ 0 & \text{if } \tau_{s} < t < BCL \end{cases}$$

where I_{stim} is the stimulation strength, τ_s is the stimulation duration and BCL is the pacing period of the AP cycle.

For this piecewise nature of the stimulation signal, we consider two different modes for voltage dynamics in the HA: 1) stimulus mode and 2) non-stimulus mode. Since the dynamics of variable h is also defined as a piece-wise function in Eq. (1), we can represent the MS cardiac-cell model as a four-mode hybrid automaton (HA), as shown in Fig. 2(a). We add an additional state variable τ that serves as a local clock for time-triggered events; for example, the transition from a stimulus to a non-stimulus mode or the transition from the current AP cycle to the next.

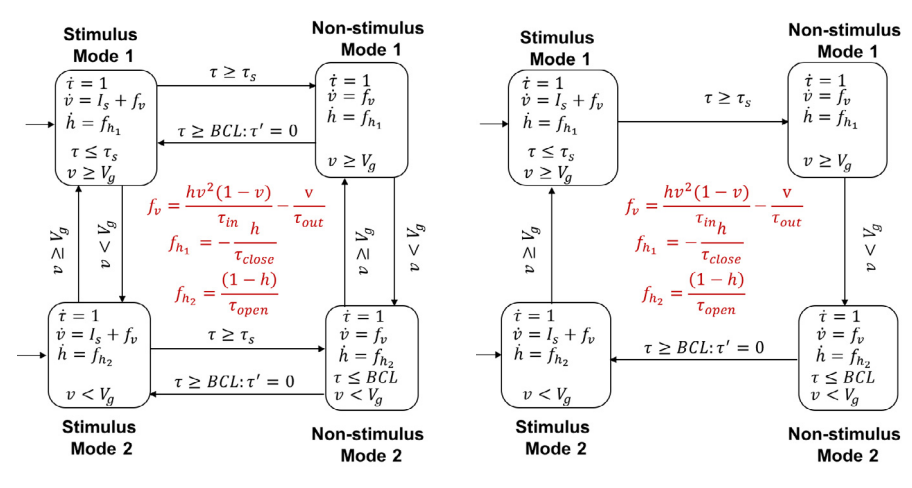
Depending on the parameter values, stimulation signal and pacing period, the HA in Fig. 2(a) can generate either an AP signal or no AP signal. As we are interested in analyzing alternans in this paper, we can simplify the HA by considering the situation when it will always generate the AP signal in each cycle. As the AP signal satisfies the following criteria, we can simplify this HA by removing certain edges:

- $v < V_g$ will not occur in "Stimulus Mode 1", as the value of v always increases in this mode
- $v \ge V_g$ will not occur in "Non-stimulus Mode 2", as v always decreases in this mode
- $v \ge V_g$ occurs before $\tau \ge \tau_s$ in "Stimulus Mode 2"
- For a chosen BCL range, $v < V_g$ occurs before $\tau \ge BCL$ in "Non-stimulus Mode 1"

Fig. 2(b) shows our simplified cellular HA, \mathcal{H}_M .

3.2. Encoding alternans and non-alternans as hybrid automata

We generalize the classical definition of alternans that incorporates transient cycles and a tolerance threshold r_{th} , $0 \le r_{th} \le 1$, which establishes the relative difference between APDs. Transients are important since, when starting from an initial



(a) Detailed MS Automaton

(b) Simplified MS Automaton \mathcal{H}_M

Fig. 2. The four-mode hybrid automaton for the MS model. The primed version of variables is used to indicate the reset map of a given transition. Variables not shown in the reset map are not updated during the jump.

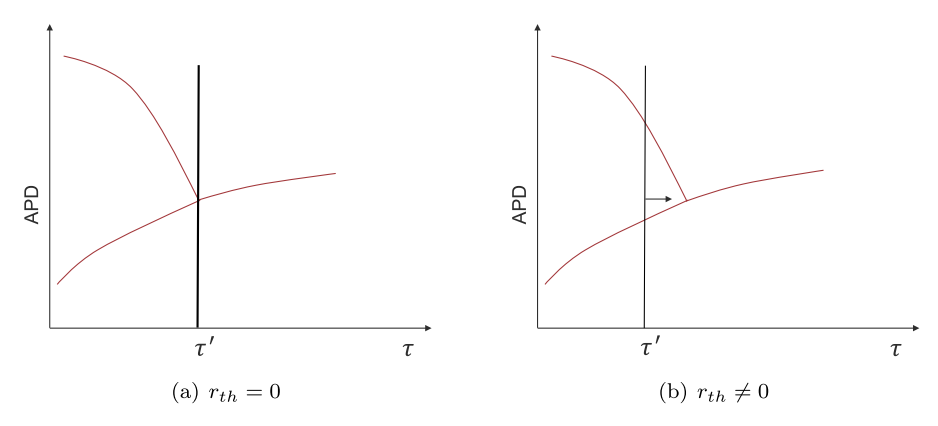


Fig. 3. Effect of r_{th} on bifurcation point.

state and a set of parameters that are known to produce alternans, the voltage signal only settles into period-doubling after the transient phase is over. Failure to incorporate transient cycles can result in unwanted effects on the alternans calculation. We add the tolerance threshold r_{th} to take into account noise and measurement errors in the clinical data that is used to calculate alternans.

Definition 1. Let σ be a (possibly infinite) voltage signal that begins with N_{trans} AP cycles, followed by at least two AP cycles, where N_{trans} is the number of transient cycles. Let $\tau_1 > 0$ and $\tau_2 > 0$ be the APDs of any two consecutive AP cycles after the initial N_{trans} cycles in σ . Further, let $r = \frac{\tau_2}{\tau_1}$. We say that σ exhibits alternans with respect to a given r_{th} when $|r-1| > r_{th}$ is an invariant. Likewise, we say that σ exhibits non-alternans with respect to r_{th} when $|r-1| \le r_{th}$ is an invariant.

Remark 1. As opposed to using the absolute value of the difference of consecutive APDs $(|APD_1 - APD_2|)$ for the definition of alternans, Definition 1 yields a *normalized* (between 0 and 1) basis for comparison. Note that as r_{th} is increased, the estimated bifurcation point is moved away from the exact value and farther into the alternans region. In the limit as r_{th} approaches zero, the estimated bifurcation point approaches the exact value, as shown in Fig. 3. Note that, when $r_th = 0$, the definition yields classical alternans.

Remark 2. The value of N_{trans} is typically small and chosen based on the domain knowledge. Although a small quantitative difference may occur, there is no qualitative difference in the state trajectories for two different nonzero values of N_{trans} . Thus, the impact on alternans computation is negligible even when N_{trans} is chosen as a small number.

For encoding purpose, we consider alternans as a safety property and then characterize it using a so-called *safety automaton* [2]. For our purposes, a safety automaton is an HA with modes additionally marked as *accepting* or *non-accepting*,

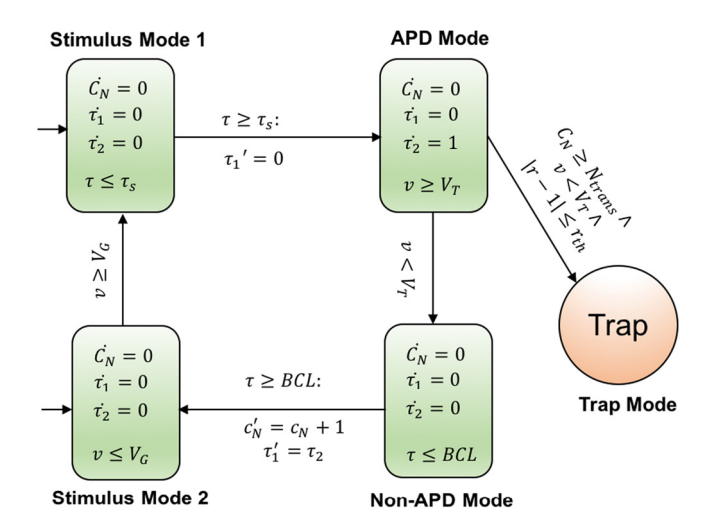


Fig. 4. The hybrid automaton \mathcal{H}_0 for the observer. The number after the colon in each mode name gives a number to the mode. Mode "Trap" is non-accepting; all other modes are accepting.

and with the property that no accepting mode can be reaching from a non-accepting mode. After first determining that \mathcal{H}_M has completed N_{trans} transient cycles, our safety, or *observer*, automaton \mathcal{H}_0 repeatedly computes two successive APDs τ_1 and τ_2 , and checks if the condition for alternans (Definition 1) is violated. If so, the automaton enters a trap (i.e. non-accepting) state, from which it never exits. If no such violation is detected, then the observed sequence of cycles is accepted. Thus, in \mathcal{H}_0 , there is a single non-accepting mode named "Trap"; all other modes are accepting. Note that \mathcal{H}_0 uses the v and τ values from \mathcal{H}_M to determine when a cycle has completed and to compute APD values.

Fig. 4 presents observer automaton \mathcal{H}_0 for the alternans problem. As, by definition, APD is the time period in each AP cycle during which $v \geq V_T$, V_T is a small positive constant and typically same as V_G in the MS model, an APD event can occur only in "Stimulus Mode 1" and "Non-stimulus Mode 1" in \mathcal{H}_M . As the "Stimulus Mode 1" is at most τ_S and τ_S (typically 1 ms) is negligible compared to the duration of "Non-stimulus Mode 1" (> 200 ms), we ignore the event $v \geq V_T$ inside "Stimulus Mode 1" to avoid more modes in \mathcal{H}_0 . By considering $V_T = V_G$, we could further reduce another mode in \mathcal{H}_0 . So the APD is computed by the duration \mathcal{H}_M remains at "Non-stimulus Mode 1".

To compute APD in two consecutive cycles, we add two clock variables: 1) τ_1 which holds the APD in previous cycle and 2) τ_2 which holds the APD of current cycle. In each cycle, before entering "APD Mode", τ_2 is reset and is kept active only during this mode. Though τ_1 is always inactive, it is reset to the value of τ_2 before starting the next cycle so that it can contain the APD of previous cycle.

To determine whether \mathcal{H}_M completes N_{trans} transient cycles, we add a counter C_N in \mathcal{H}_0 which is increased by 1 during the jump from "Non-APD Mode" to "Stimulus Mode 2". In $(N_{trans}+1)$ -th cycle, when $v < V_T \land |r-1| \le r_{th}$ holds, a transition from "APD Mode" to "Trap Mode" occurs, i.e., the alternans occurs. All the other modes are the accepting states for this safety (Büchi) automaton.

To check the alternans property, we combine \mathcal{H}_M and \mathcal{H}_0 into a single automaton \mathcal{H}_A as shown in Fig. 5. This approach is known as shared-variable composition [5]. Let Θ_0 be a set of initial states in \mathcal{H}_A . We say Θ_0 produce alternans when:

$$\exists \theta_0 \in \Theta_0$$
. "Trap Mode" is reachable in \mathcal{H}_A . (2)

4. Bifurcation analysis of alternans using sReach

In this section, we present a probabilistic reachability based algorithm for multi-parameter bifurcation analysis of cardiac alternans using the hybrid automaton \mathcal{H}_A .

Definition 2. Assume $\mathcal{T}_{all} = \{\tau_1, \tau_2, ..., \tau_n\}$ is the set of all control parameters in the MS model. The bounded parameter space for a subset $\mathcal{T} \subseteq \mathcal{T}_{all}$ is defined as $B_{\mathcal{T}} = [\underline{\tau_1}, \overline{\tau_1}] \times [\underline{\tau_2}, \overline{\tau_2}] \times \cdots \times [\underline{\tau_m}, \overline{\tau_m}]$, where the cardinality of $|\mathcal{T}| = m$, $m \le n$. We define the *multi-parameter bifurcation analysis* of cardiac alternans for the subset \mathcal{T} as finding the *bifurcation hypersurface* (BH) in $B_{\mathcal{T}}$ such that a small perturbation to this hypersurface results in transition from alternans to non-alternans behavior or vice-versa.

In [26], we presented a reachability-based method for this problem when $|\mathcal{T}| = 1$. Solving reachability problem for general hybrid systems is undecidable [3]. Therefore, we relaxed the reachability problem by a technique that utilizes a δ -decision procedure. Though, due to the δ -relaxation, our presented method could not compute the exact bifurcation point (BP), it bounded the BP into a tighter region. In this paper, we also compute a tighter bounded region that contains the

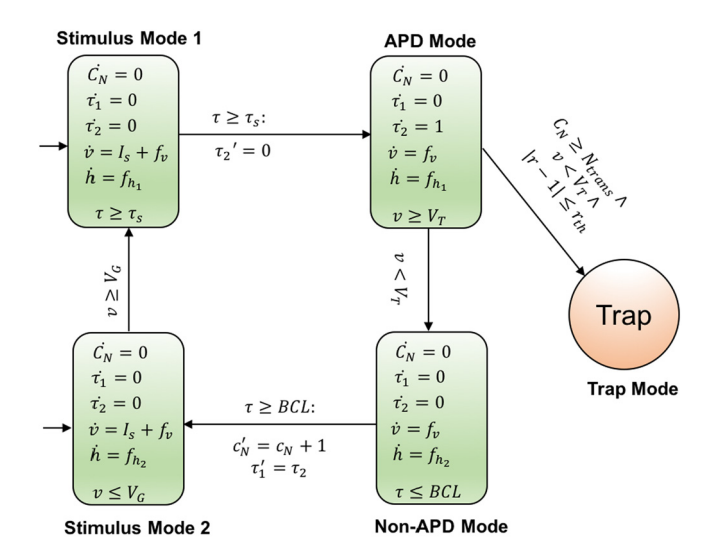


Fig. 5. The 5-mode hybrid automaton \mathcal{H}_A for alternans.

Algorithm 1 Multi-parameter bifurcation analysis on sReach.

```
1: global variables
 2:
          AR, NR, BR
 3: end global variables
  4: procedure Bifurcation-Analysis(\mathcal{T}, B_{\mathcal{T}}, \delta_0, P_l, P_h)
 5:
          AR \leftarrow \{\} \quad NR \leftarrow \{\} \quad BR \leftarrow B_{\mathcal{T}} \quad \delta \leftarrow \delta_0
 6:
          iter \leftarrow 0
          k \leftarrow 4N_{trans} + 3
  7:
 8:
          repeat
 9:
               RecursiveSearch(\mathcal{T}, B_{\mathcal{T}}, \delta, P_l, P_h, k)
10:
               Decrease δ
11:
               iter \leftarrow iter + 1
          until BR meets desired precision criteria or iter \leq MAXITER
12:
13: end procedure
```

```
1: procedure RecursiveSearch(\mathcal{T}, B_{\mathcal{T}}, \delta, P_l, P_h, k)
 2:
            if |B_{\mathcal{T}}| \leq |B_{\delta}| then
 3:
                   BR \leftarrow B_{\mathcal{T}} \cup BR
 4:
                   return
 5:
            end if
 6:
             \tilde{P} \leftarrow sReach(\mathcal{H}_A, \mathcal{T}, B_{\mathcal{T}}, \delta, k)
  7:
            if \tilde{P} > P_h then
 8:
                  AR \leftarrow B_{\mathcal{T}} \cup AR
 9:
                   return
10:
             end if
11:
             if \tilde{P} < P_l then
                   NR \leftarrow B_{\mathcal{T}} \cup NR
12:
13:
                   return
             end if
14.
15:
             (B_{\mathcal{T}}^l, B_{\mathcal{T}}^r) \leftarrow \text{BISECT}(B_{\mathcal{T}})
             RecursiveSearch(\mathcal{T}, B_{\mathcal{T}}^{l}, \delta, P_{l}, P_{h}, k)
16:
17:
             RECURSIVESEARCH(\mathcal{T}, B_{\mathcal{T}}^{r'}, \delta, P_l, P_h, k)
18: end procedure
```

BH for $|\mathcal{T}| > 1$. As our previous method is not scalable in multi-parameter setting, we solve this problem by employing the probabilistic reachability analysis based technique that combines the δ -decision procedure with statistical tests. Algorithm 1 serves as an outline of our bifurcation analysis of alternans for \mathcal{T} . The algorithm terminates when the size of the BR meets a user-desired precision criteria or the loop iterates to a certain number of times defined by *MAXITER*.

Algorithm 1 starts by defining three global variables: AR (Alternans Region), NR (Non-alternans Region), and BR (Bifurcation Region). At the beginning, we assume the entire parameter space $B_{\mathcal{T}}$ as BR and iteratively refine it in the repeat-until block. While refining BR, we also update AR and NR appropriately.

As the sReach tool is a bounded-time reachability analysis tool, it requires a bound on the number of unrolling, k. In line 7, we added a equation to compute k using N_{trans} . Here 4 is the number of jump to complete one cycle and 3 is the maximum number of jump to go from initial mode to the trap mode.

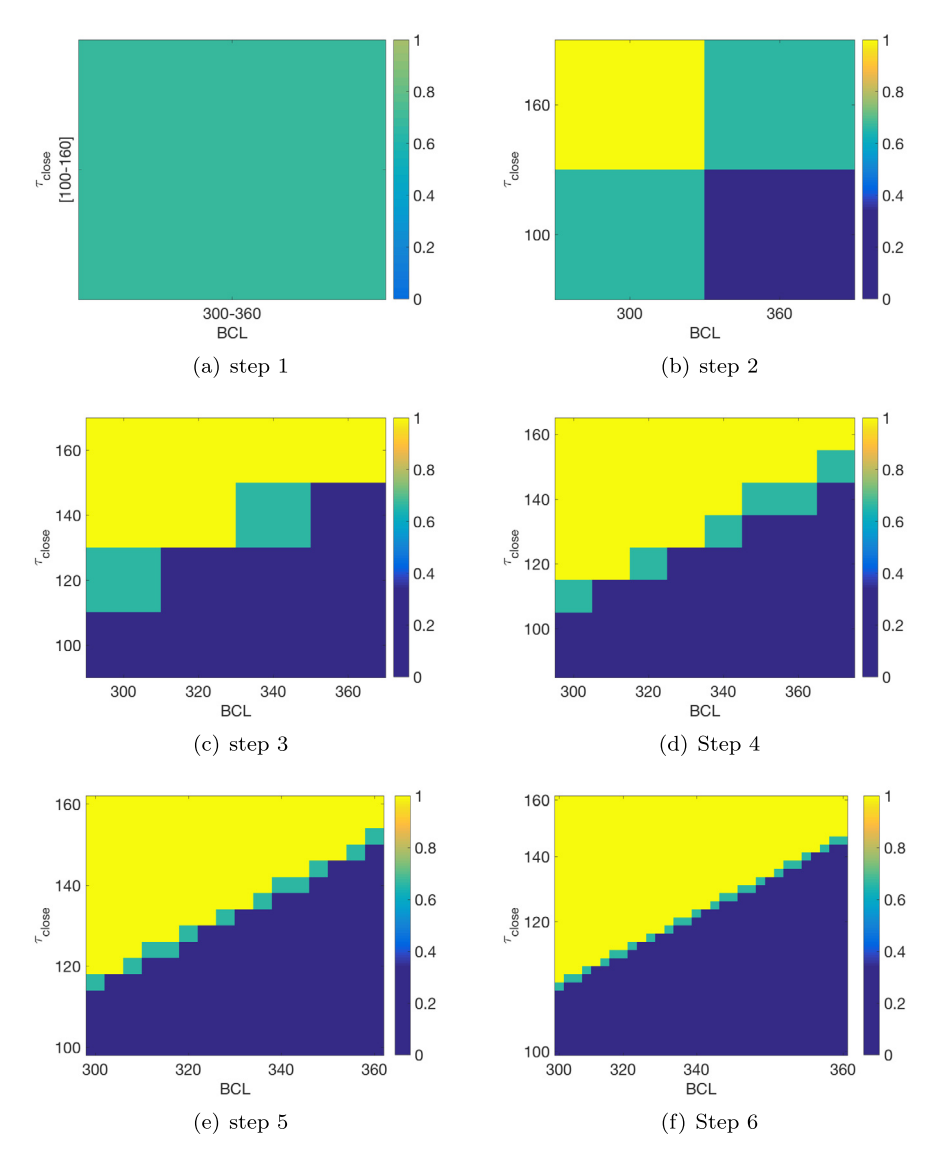


Fig. 6. A demonstration of the recursive search procedure of Algorithm 1. The yellow, blue and green regions represent AR, NR and BR, respectively. (For interpretation of the references to color in this figure, the reader is referred to the web version of this article.)

In the repeat-until block, we call a recursive search procedure that takes \mathcal{T} , $B_{\mathcal{T}}$, a δ value used by the δ -decision procedure in the sReach tool and two user-defined upper and lower probability thresholds P_l and P_h . The recursive search algorithm first checks whether $B_{\mathcal{T}}$ reaches the minimum size defined by $|B_{\delta}| = \delta^m$ such that $\forall i \in \{1, 2, \dots, m\}, |\bar{\tau}_i - \underline{\tau}_i| \leq \delta$, where $|\mathcal{T}| = m$. If $|B_{\mathcal{T}}| > |B_{\delta}|$, the method runs the sReach script and estimate the probability \tilde{P} at which $B_{\mathcal{T}}$ produces alternans. If $\tilde{P} > P_h$, it adds $B_{\mathcal{T}}$ to AR and returns. It adds $B_{\mathcal{T}}$ to NR, when $\tilde{P} < P_l$. The algorithm bisect $B_{\mathcal{T}}$, when $\tilde{P} \in [P_l, P_h]$ and recursively calls both left and right half of $B_{\mathcal{T}}$.

Remark 3. In BISECT subroutine, we randomly choose only one parameter with range greater than δ and bisect the parameter space along that dimension only.

Fig. 6 demonstrates the iterative steps of Algorithm 1. At first step, the entire box is green (BR), as $\tilde{P} \in [0.15, 0.85]$. In the next step, the upper-left box becomes yellow (AR) and lower-right box becomes blue (NR), but the other two boxes remain green. The algorithm continues until the green boxes reaches a minimum size defined by the precision criteria.

4.1. Complexity and correctness of Algorithm 1

The complexity and correctness of the algorithm depends on the desired precision criteria, i.e., the termination criteria, and the DFS-like recursive search procedure and underlying δ -decision procedure and statistical tests.

4.1.1. Complexity

The *repeat-until* loop in Algorithm 1, depending on the precision criteria, iterates at most *MAXITER* times, a predefined maximum iterator. At each iteration, we run the recursive procedure to find the BH for a fixed δ value that is used in the δ -decision procedure.

The number of the iteration in the recursive-search method depends on size of $|B_{\mathcal{T}}|$ and $|B_{\delta}|$, where $|B_{\delta}| = \delta^{|\mathcal{T}|}$. In worst case, the number of iteration $m = lg(\frac{|B_{\mathcal{T}}|}{|B_{\delta}|})$.

At each iteration of the recursive-search method, except in the base case, the sReach tool estimates the probability \tilde{P} for the parameter-space $B_{\mathcal{T}}$. The runtime of this step depends on the underlying sampling method, δ -decision procedure and number of samples determined by statistical tester.

For the sampling part, the complexity is linear to the number of parameters $|\mathcal{T}|$ used in the multi-parametric bifurcation analysis. For statistical testing part, when the Bayesian estimation method is applied, the complexity of is also a linear function over the chosen error bound and parameters α and β [49].

To analyze the complexity of δ -decision procedure, let us consider \mathcal{F} is a set of Lipschitz-continuous ODEs over compact domain. In [32], Kong et al. shows that the hybrid automaton can be encoded as a sentence in first-order logic over the reals, $\mathcal{L}_{\mathbb{R}_{\mathcal{F}}}$. The δ -decision problem for a bounded sentence of $\mathcal{L}_{\mathbb{R}_{\mathcal{F}}}$ is PSPACE-complete [21].

To summarize, Algorithm 1 has a nested loop structure that runs for a finite number of iterations ($MAXITER \times m$), where each iteration in the inner loop is PSPACE-complete due to the underlying δ -decision procedure. As PSPACE-complete is close under union, complementation and Kleene star, the overall complexity of Algorithm 1 is also PSPACE-complete.

4.1.2. Correctness

Our algorithm determines the BH using a recursive search method. At each iteration of the search procedure, we apply the sReach tool to estimate the probability that the current region contains the BH. Thus, the correctness of our algorithm depends on the correctness of the sReach tool.

Since SReach combines δ -decision procedure with sampling and statistical tests, it sacrifices the soundness for the scalability, which is similar to statistical model checking [34] and other simulation-based methods. However, the estimation error in the sReach can be bound in two ways: 1) user-defined error controlling parameters of the statistical tester method and 2) the estimation of Bernoulli distribution, estimated according to the δ -sat results of the dReach, passed to the statistical tester. Thus the correctness of our algorithm is ensured by the underlying statistical testing method and δ -decision procedure in the sReach tool.

5. Results

In this section, we present the results of performing bifurcation analysis of alternans over several combinations of two and three parameters of the MS model using Algorithm 1. When we performed bifurcation analysis for a subset of parameters, we fixed the other parameter as follows: $[V_G, r_{th}, N_{trans}, BCL, \tau_{in}, \tau_{out}, \tau_{open}, \tau_{close}]$ were set to [0.15, 0.01, 1, 300, 0.3, 6, 20, 150] unless specified otherwise. As we were interested only in the parameter variation, we fixed the initial condition for \mathcal{H}_A with v(0) = 0.2, h(0) = 1 with $C_N(0)$, $\tau(0)$, $\tau(0)$ and $\tau_2(0)$ all set to zero. In all cases, we considered the voltage signal with $N_{trans} + 2$ AP cycles. The parameter ranges considered during the bifurcation analysis are as follows: $BCL \in [300, 360]$, $\tau_{in} \in [0.3, 0.6]$, $\tau_{out} \in [3, 6]$, $\tau_{open} \in [20, 30]$ and $\tau_{close} \in [100, 160]$. In our experiments, we used 0.01 for δ_0 and Bayesian sequential estimation with 0.05 half-interval width, coverage probability 0.99, and uniform prior $(\alpha = \beta = 1)$ for statistical tests for the sReach tool.

Remark 4. As described in Remark 2, the value of N_{trans} does not have much impact on alternans computation. To reduce the computation time in sReach, we thus choose its value as 1.

Fig. 7 illustrates several combinations of two-parameter bifurcation analysis of alternans in the MS model using Algorithm 1. From the figure, we can observe that the lower-values for BCL and τ_{in} and the upper-values for τ_{out} and τ_{close} favors the alternans behavior, whereas the chosen range of τ_{open} almost always produces alternans behavior. All of our findings support the analysis made Mitchell et al. in [39].

Fig. 8 illustrates our bifurcation analysis for several combinations of three parameters of the MS model. From the figure, it is clear that the size of alternans region increases in the cases when τ_{open} is used in \mathcal{T} . However, this 3-parameter analysis shows that effect of τ_{open} in producing alternans can be reduced by varying another parameters. Fig. 8 (a) shows that our algorithm is able to detect more than one bifurcation region, if $B_{\mathcal{T}}$ contains more than one bifurcation hypersurfaces.

From both 2- and 3-parameter analysis, we notice that both timing constants for the gating variable h are critical in producing alternans. In particular, τ_{open} is the most sensitive parameter, a small perturbation to it from the nominal value produces alternans. This finding is consistent with the result found in the experimental study performed in [12], where it is shown that the opening and closing of h-gate plays a critical role in producing cellular alternans.

6. Related work

Reachability analysis has emerged as a promising solution for many biological systems [7,51,27,17]. SMT-based verification using dReal [20] has been applied in various problems [41,28,31,6,10,42]. Liu et al. successfully applied SMT-based

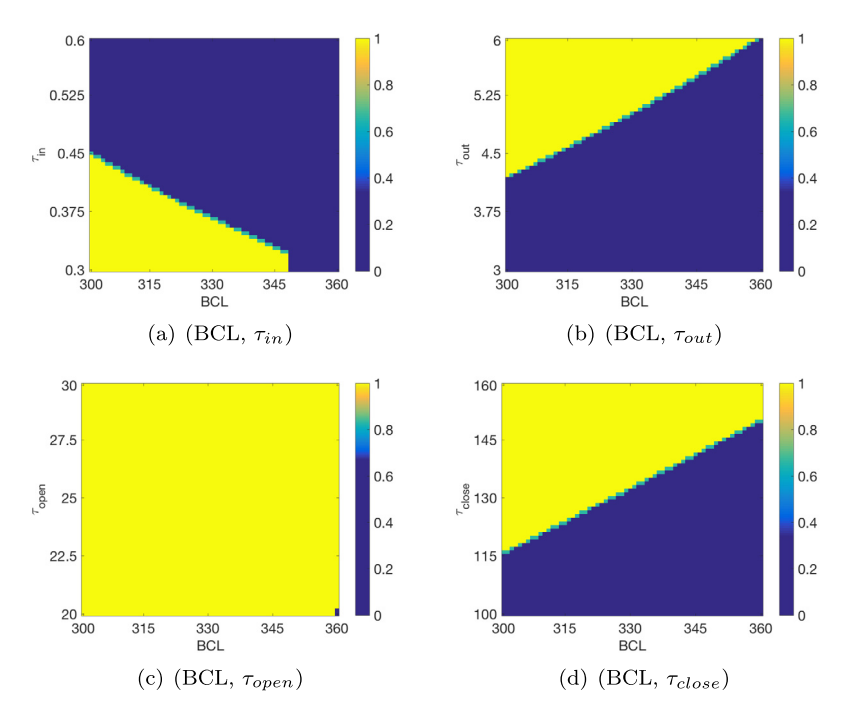


Fig. 7. Two-parameter bifurcation analysis of alternans in the MS model. The yellow, blue and green regions represent alternans, non-alternans and bifurcation regions, respectively. (For interpretation of the references to color in this figure legend, the reader is referred to the web version of this article.)

reachability analysis using dReach in identifying patient-specific androgen ablation therapy schedules for postponing the potential cancer relapse in [35].

Brim et al. present a bifurcation analysis technique to analyze stability of genetic regulatory networks in [9]. They first express various stability-related properties by a temporal logic language extended by directional propositions and then verify those properties by varying the model parameters. Even though they apply their method only on piece-wise affine dynamics, the authors claim that it can be extended for piece-wise multiaffine dynamics. The method, however, is not applicable to general nonlinear dynamical systems.

In [24], Huang et al. presents a reachability analysis technique for a hybrid model of cardiac dynamics for a 1-d cable of cells and show the presence of alternans based on computed reachtube. The authors, however, neither define nor verify the alternans property formally. They just do reachability analysis for two *BCL* values and show, by visual inspection, that one *BCL* value produces alternans and another does not.

7. Conclusions

In this paper, we have applied probabilistic-reachability analysis to identify the bifurcation hypersurfaces that represent the transition to alternans in the Mitchell–Schaeffer cardiac-cell model. Our bifurcation analysis is performed using the probabilistic-reachability tool sReach [49], and uses a sophisticated guided-search strategy to "zoom in" on the bifurcation hypersurface in question. Since this tool is designed to work with nonlinear hybrid systems, we converted the original MS model into a hybrid automaton (HA), and further extended this HA to encode alternans-like behavior.

For future work, we intend to study other models where alternans are not due to solely the voltage dynamics, as in the MS model. Rather, they may also be caused by the calcium dynamics, as both mechanisms have been found to occur in cardiac cells [46].

We also plan to extend the cell-level bifurcation analysis we conducted to a 1-d cable of cells. Traveling waves can exhibit alternans along cables [50]. Doing so, will require us to extend our reachability analysis from ODEs to PDEs. We can also extend our analysis by varying multiple parameters simultaneously; currently, we only vary one parameter at a time. We can accomplish this by augmenting the state vector with each of these parameters.

Acknowledgments

We would like to thank the anonymous reviewers for their helpful comments. Research supported in part by the following grants: NSF IIS-1447549, NSF CPS-1446832, NSF CPS-1446725, NSF CNS-1446665, NSF CPS 1446365, NSF CAR 1054247, AFOSR FA9550-14-1-0261, AFOSR YIP FA9550-12-1-0336, CCF-0926190, ONR N00014-13-1-0090, and NASA NNX12AN15H.

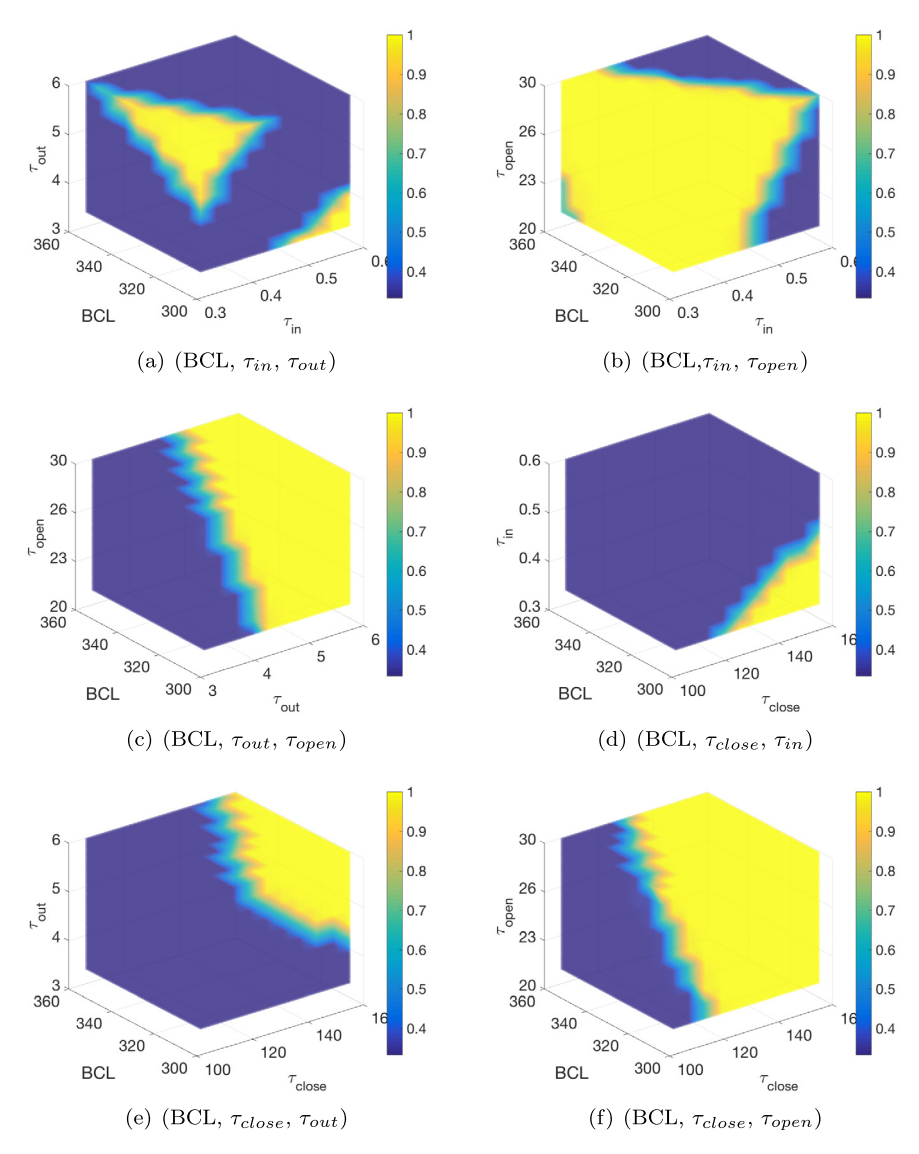


Fig. 8. Three-parameter bifurcation analysis of alternans in the MS model. The yellow, dark-blue and light-blue regions represent alternans, non-alternans and bifurcation regions, respectively. (For interpretation of the references to color in this figure legend, the reader is referred to the web version of this article.)

References

- [1] A. Shrier, H. Dubarsky, M. Rosengarten, M.R. Guevara, S. Nattel, L. Glass, Prediction of complex atrioventricular conduction rhythms in humans with use of the atrioventricular nodal recovery curve, Circulation 76 (6) (Dec. 1987) 1196–1205.
- [2] B. Alpern, F.B. Schneider, Recognizing safety and liveness, Distrib. Comput. 2 (3) (1987) 117–126.
- [3] R. Alur, C. Courcoubetis, N. Halbwachs, T.A. Henzinger, P.-H. Ho, X. Nicollin, A. Olivero, J. Sifakis, S. Yovine, The algorithmic analysis of hybrid systems, Theoret. Comput. Sci. 138 (1) (1995) 3–34.
- [4] R. Alur, C. Courcoubetis, T.A. Henzinger, P. Ho, Hybrid automata: an algorithmic approach to the specification and verification of hybrid systems, in: Hybrid Systems, 1992, pp. 209–229.
- [5] R. Alur, T.A. Henzinger, P.-H. Ho, Automatic symbolic verification of embedded systems, IEEE Trans. Softw. Eng. 22 (3) (1996) 181-201.
- [6] K. Bae, P.C. Ölveczky, S. Kong, S. Gao, E.M. Clarke, SMT-based analysis of virtually synchronous distributed hybrid systems, in: Proceedings of the 19th International Conference on Hybrid Systems: Computation and Control, ACM, 2016, pp. 145–154.
- [7] G. Batt, H. De Jong, M. Page, J. Geiselmann, Symbolic reachability analysis of genetic regulatory networks using discrete abstractions, Automatica 44 (4) (2008) 982–989.
- [8] G.E. Billman, Cardiac autonomic neural remodeling and susceptibility to sudden cardiac death: effect of endurance exercise training, Am. J. Physiol. Heart Circ. Physiol. 297 (4) (2009) H1171–H1193.
- [9] L. Brim, M. Demko, S. Pastva, D. Šafránek, High-performance discrete bifurcation analysis for piecewise-affine dynamical systems, in: Hybrid Systems Biology, Springer, 2015, pp. 58–74.
- [10] D. Bryce, S. Gao, D.J. Musliner, R.P. Goldman, SMT-based nonlinear PDDL+ planning, in: 29th AAAI Conference on Artificial Intelligence, 2015, p. 3247.
- [11] J.-M. Cao, Z. Qu, Y.-H. Kim, T.-J. Wu, A. Garfinkel, J.N. Weiss, H.S. Karagueuzian, P.-S. Chen, Spatiotemporal heterogeneity in the induction of ventricular fibrillation by rapid pacing, Circ. Res. 84 (11) (1999) 1318–1331.

- [12] D.D. Chen, R.A. Gray, I. Uzelac, C. Herndon, F.H. Fenton, Mechanism for amplitude alternans in electrocardiograms and the initiation of spatiotemporal chaos, Phys. Rev. Lett. 118 (16) (2017) 168101.
- [13] S.J. Connolly, M. Gent, R.S. Roberts, P. Dorian, D. Roy, R.S. Sheldon, L.B. Mitchell, M.S. Green, G.J. Klein, B. O'brien, et al., Canadian implantable defibrillator study (CIDS), Circulation 101 (11) (2000) 1297–1302.
- [14] A.R. Cram, H.M. Rao, E.G. Tolkacheva, Toward prediction of the local onset of alternans in the heart, Biophys. J. 100 (4) (2011) 868-874.
- [15] F.H. Fenton, E.M. Cherry, H.M. Hastings, M. Harold, S.J. Evans, Multiple mechanisms of spiral wave breakup in a model of cardiac electrical activity, Chaos 12 (3) (2002) 852.
- [16] F.H. Fenton, E.M. Cherry, Models of cardiac cell, Scholarpedia 3 (8) (2008) 1868.
- [17] J. Feret, Reachability analysis of biological signalling pathways by abstract interpretation, in: Computation in Modern Science and Engineering, Volume 2, Part A, in: AIP Conference Proceedings, vol. 963, 2007, pp. 619–622.
- [18] S. Gao, J. Avigad, E.M. Clarke, Delta-complete decision procedures for satisfiability over the reals, in: Proceedings of the 6th International Joint Conference on Automated Reasoning, IJCAR'12, Springer-Verlag, Berlin, Heidelberg, 2012, pp. 286–300.
- [19] S. Gao, S. Kong, W. Chen, E.M. Clarke, Delta-complete analysis for bounded reachability of hybrid systems, CoRR, arXiv:1404.7171, 2014.
- [20] S. Gao, S. Kong, E.M. Clarke, dReal: an SMT solver for nonlinear theories over the reals, in: Automated Deduction CADE-24, Springer, 2013, pp. 208–214.
- [21] S. Gao, S. Kong, E.M. Clarke, dReal: an SMT solver for nonlinear theories over the reals, in: Automated Deduction CADE-24 24th International Conference on Automated Deduction. Proceedings, Lake Placid, NY, USA, June 9–14, 2013, 2013, pp. 208–214.
- [22] A. Gizzi, E.M. Cherry, R.F. Gilmour Jr, S. Luther, S. Filippi, F.H. Fenton, Effects of pacing site and stimulation history on alternans dynamics and the development of complex spatiotemporal patterns in cardiac tissue, Front. Physiol. 4 (2013) 71.
- [23] M.E. Henderson, Multiple parameter continuation: computing implicitly defined k-manifolds, Internat. J. Bifurc. Chaos 12 (03) (2002) 451-476.
- [24] Z. Huang, C. Fan, A. Mereacre, S. Mitra, M. Kwiatkowska, Invariant verification of nonlinear hybrid automata networks of cardiac cells, in: Proceedings of 26th International Conference on Computer Aided Verification (CAV), in: Lecture Notes in Comput. Sci., vol. 8559, Springer, 2014, pp. 373–390.
- [25] T. Ikeda, H. Saito, K. Tanno, H. Shimizu, J. Watanabe, Y. Ohnishi, Y. Kasamaki, Y. Ozawa, T-wave alternans as a predictor for sudden cardiac death after myocardial infarction, Am. J. Cardiol. 89 (1) (2002) 79–82.
- [26] M.A. Islam, G. Byrne, S. Kong, E.M. Clarke, R. Cleaveland, F.H. Fenton, R. Grosu, P.L. Jones, S.A. Smolka, Bifurcation analysis of cardiac alternans using δ-decidability, in: International Conference on Computational Methods in Systems Biology, Springer, 2016, pp. 132–146.
- [27] M.A. Islam, R. De Francisco, C. Fan, R. Grosu, S. Mitra, S.A. Smolka, Model checking tap withdrawal in C. Elegans, in: Hybrid Systems Biology, 2015, p. 195.
- [28] M.A. Islam, A. Murthy, A. Girard, S.A. Smolka, R. Grosu, Compositionality results for cardiac cell dynamics, in: Proceedings of the 17th International Conference on Hybrid Systems: Computation and Control, ACM, 2014, pp. 243–252.
- [29] J.B. Nolasco, R.W. Dahlen, A graphic method for the study of alternation in cardiac action potentials, J. Appl. Physiol. 25 (2) (Aug. 1968) 191-196.
- [30] J.N. Weiss, S. Alain, Y. Shiferaw, P. Chen, A. Garfinkel, Z. Qu, From pulsus to pulseless: the saga of cardiac alternans, Circ. Res. 98 (10) (May 2006) 1244–1253, WOS:000237812200006.
- [31] J. Kapinski, J.V. Deshmukh, S. Sankaranarayanan, N. Arechiga, Simulation-guided Lyapunov analysis for hybrid dynamical systems, in: Hybrid Systems: Computation and Control (HSCC), ACM Press, 2014, pp. 133–142.
- [32] S. Kong, S. Gao, W. Chen, E.M. Clarke, dReach: δ-reachability analysis for hybrid systems, in: Tools and Algorithms for the Construction and Analysis of Systems 21st International Conference, TACAS. Proceedings, London, UK, April 11–18, 2015, 2015, pp. 200–205.
- [33] K.-H. Kuck, R. Cappato, J. Siebels, R. Rüppel, et al., Randomized comparison of antiarrhythmic drug therapy with implantable defibrillators in patients resuscitated from cardiac arrest, Circulation 102 (7) (2000) 748–754.
- [34] A. Legay, B. Delahaye, S. Bensalem, Statistical model checking: an overview, in: RV, vol. 10, 2010, pp. 122-135.
- [35] B. Liu, S. Kong, S. Gao, P. Zuliani, E.M. Clarke, Towards personalized prostate cancer therapy using delta-reachability analysis, in: Proceedings of the 18th International Conference on Hybrid Systems: Computation and Control, ACM, 2015, pp. 227–232.
- [36] M. Guevara, L. Glass, A. Shrier, Phase locking, period-doubling bifurcations, and irregular dynamics in periodically stimulated cardiac cells, Science 214 (4527) (Dec. 1981) 1350–1353.
- [37] J. McAnulty, B. Halperin, J. Kron, G. Larsen, M. Rait, R. Swenson, R. Floreck, C. Marchant, M. Hamlin, G. Heywood, et al., A comparison of antiarrhythmic-drug therapy with implantable defibrillators in patients resuscitated from near-fatal ventricular arrhythmias, N. Engl. J. Med. 337 (22) (1997) 1576–1583.
- [38] Task Force Members, V. Fuster, L.E. Rydén, D.S. Cannom, H.J. Crijns, A.B. Curtis, K.A. Ellenbogen, J.L. Halperin, J.-Y. Le Heuzey, G.N. Kay, et al., ACC/AHA/ESC 2006 guidelines for the management of patients with atrial fibrillation—executive summary: a report of the American College of Cardiology/American Heart Association Task Force on practice guidelines and the European Society of Cardiology Committee for Practice Guidelines (writing committee to revise the 2001 guidelines for the management of patients with atrial fibrillation) developed in collaboration with the European Heart Rhythm Association and the Heart Rhythm Society, Eur. Heart J. 27 (16) (2006) 1979–2030.
- [39] C.C. Mitchell, D.G. Schaeffer, A two-current model for the dynamics of cardiac membrane, Bull. Math. Biol. 65 (5) (2003) 767-793.
- [40] A.J. Moss, W.J. Hall, D.S. Cannom, J.P. Daubert, S.L. Higgins, H. Klein, J.H. Levine, S. Saksena, A.L. Waldo, D. Wilber, et al., Improved survival with an implanted defibrillator in patients with coronary disease at high risk for ventricular arrhythmia, N. Engl. J. Med. 335 (26) (1996) 1933–1940.
- [41] A. Murthy, M.A. Islam, S.A. Smolka, R. Grosu, Computing bisimulation functions using SOS optimization and δ -decidability over the reals, in: Proceedings of the 18th International Conference on Hybrid Systems: Computation and Control, ACM, 2015, pp. 78–87.
- [42] A. Murthy, M.A. Islam, S.A. Smolka, R. Grosu, Computing compositional proofs of input-to-output stability using SOS optimization and δ-decidability, Nonlinear Anal. Hybrid Syst. 23 (2017) 272–286.
- [43] S.M. Narayan, D.E. Krummen, K. Shivkumar, P. Clopton, W.-J. Rappel, J.M. Miller, Treatment of atrial fibrillation by the ablation of localized sources: confirm (conventional ablation for atrial fibrillation with or without focal impulse and rotor modulation) trial, J. Am. Coll. Cardiol. 60 (7) (2012) 628–636.
- [44] J.M. Pastore, S.D. Girouard, K.R. Laurita, F.G. Akar, D.S. Rosenbaum, Mechanism linking t-wave alternans to the genesis of cardiac fibrillation, Circulation 99 (10) (1999) 1385–1394.
- [45] R.F. Gilmour, D.R. Chialvo, Electrical restitution, critical mass, and the riddle of fibrillation, J. Cardiovasc. Electrophysiol. 10 (8) (Aug. 1999) 1087–1089.
- [46] Y. Shiferaw, D. Sato, A. Karma, Coupled dynamics of voltage and calcium in paced cardiac cells, Phys. Rev. E 71 (2) (2005) 021903.
- [47] T. Quail, A. Shrier, L. Glass, Predicting the onset of period-doubling bifurcations in noisy cardiac systems, Proc. Natl. Acad. Sci. 112 (30) (July 2015) 9358–9363.
- [48] L. Vakulenko, Features of bioelectrical activity of the heart in children with chronic pyelonephritis, Med. Perspect. 19 (2) (2014) 85-92.
- [49] Q. Wang, P. Zuliani, S. Kong, S. Gao, E.M. Clarke Sreach, A probabilistic bounded delta-reachability analyzer for stochastic hybrid systems, in: International Conference on Computational Methods in Systems Biology, Springer, 2015.
- [50] M.A. Watanabe, F.H. Fenton, S.J. Evans, H.M. Hastings, A. Karma, Mechanisms for discordant alternans, J. Cardiovasc. Electrophysiol. 12 (2) (2001) 196–206.
- [51] Y. Yang, H. Lin, Reachability analysis based model validation in systems biology, in: Cybernetics and Intelligent Systems (CIS), 2010 IEEE Conference on, IEEE, 2010, pp. 14–19.